01 May 2003

Hyperspherical Close-Coupling Calculations for Charge-Transfer Cross Sections in He^{2+} +H(1s) Collisions At Low Energies

Chen-Nan Liu

Anh-Thu Le
Missouri University of Science and Technology, lea@mst.edu

Toru Morishita

B. D. Esry

et. al. For a complete list of authors, see https://scholarsmine.mst.edu/phys_facwork/1635

Recommended Citation

C. Liu et al., "Hyperspherical Close-Coupling Calculations for Charge-Transfer Cross Sections in He^{2+} +H(1s) Collisions At Low Energies," *Physical Review A - Atomic, Molecular, and Optical Physics*, vol. 67, no. 5, American Physical Society (APS), May 2003.
The definitive version is available at https://doi.org/10.1103/PhysRevA.67.052705

Hyperspherical close-coupling calculations for charge-transfer cross sections in $He^{2+}+H(1s)$ collisions at low energies

Chien-Nan Liu,[1,2] Anh-Thu Le,[1] Toru Morishita,[3] B. D. Esry,[1] and C. D. Lin[1]
[1]*Department of Physics, Cardwell Hall, Kansas State University, Manhattan, Kansas 66506*
[2]*Institute of Physics, National Chiao Tung University, Hsinchu 300, Taiwan*
[3]*Department of Applied Physics and Chemistry, University of Electro-Communications, 1-5-1 Chofu-ga-oka, Chofu-shi, Tokyo 182-8585, Japan*
(Received 11 December 2002; published 23 May 2003)

A theory for ion-atom collisions at low energies based on the hyperspherical close-coupling (HSCC) method is presented. In hyperspherical coordinates the wave function is expanded in analogy to the Born-Oppenheimer approximation where the adiabatic channel functions are calculated with *B*-spline basis functions while the coupled hyperradial equations are solved by a combination of *R*-matrix propagation and the slow/smooth variable discretization method. The HSCC method is applied to calculate charge-transfer cross sections for $He^{2+}+H(1s)\rightarrow He^{+}(n=2)+H^{+}$ reactions at center-of-mass energies from 10 eV to 4 keV. The results are shown to be in general good agreement with calculations based on the molecular orbital (MO) expansion method where electron translation factors (ETF's) or switching functions have been incorporated in each MO. However, discrepancies were found at very low energies. It is shown that the HSCC method can be used to study low-energy ion-atom collisions without the need to introduce the *ad hoc* ETF's, and the results are free from ambiguities associated with the traditional MO expansion approach.

DOI: 10.1103/PhysRevA.67.052705 PACS number(s): 34.70.+e, 31.15.Ja, 34.10.+x, 34.50.Pi

I. INTRODUCTION

Charge-transfer processes in slow ion-atom collisions are examples of rearrangement collisions that are difficult to treat theoretically. One of the main difficulties stems from the fact that there is not a single coordinate system that is suitable for describing all the different arrangements of the constituent particles. At low collision velocities, the electron is expected to be shared between the two slowly moving nuclei such that the collision complex can be approximated as a transient molecule. Therefore, molecular orbitals (MO's) are the natural representation for describing slow ion-atom collisions. At low energies, a full quantum mechanical treatment for both the electronic and the nuclear motion is also required. The well-known perturbed stationary state (PSS) approximation, introduced by Massey and Smith [1] more than half a century ago, is based on the MO expansion, or the adiabatic Born-Oppenheimer (BO) approximation. In the PSS model, electronic transitions occur via nonadiabatic couplings between different molecular orbitals. However, the adiabatic BO approximation is known to have severe deficiencies, originating from the fact that the molecular orbitals do not satisfy the correct asymptotic boundary conditions. The fundamental defects associated with the PSS model have been well documented, including incorrect dissociation thresholds, nonvanishing asymptotic couplings and non-Galilean-invariant calculated cross sections [2–5]. Although these problems have been well known for decades, the remedies are less obvious [6,7]. Approaches based on the so-called reaction coordinates (RC's) have been proposed [8,9], but very few calculations have been carried out [10–13]. Even within the RC method, there still exists some arbitrariness in the choice of reaction coordinates.

Most of the low-energy ion-atom collision calculations beyond the PSS model have been calculated by introducing modifications through electron translation factors (ETF's) [14,15]. The ETF's were first adopted in the semiclassical treatment of ion-atom collisions at higher energies where the internuclear motion is treated classically [16,3]. In the PSS model, the asymptotic limit of each molecular orbital is reduced to an atomic orbital. For an atom-atom or ion-atom collision, each atomic electron is supposedly moving with one or the other atom with a well-defined velocity in the asymptotic region. This translational motion is represented by attaching a plane wave ETF to each atomic orbital. Such a procedure does not specify how the translational motion should be accounted for at finite internuclear separations; thus different types of switching functions (or ETF's) have been proposed and used in actual calculations [17,18]. Such approaches are widely used in the literature and we will describe them as MO-ETF models in this paper. The introduction of ETF's in MO-ETF models means that the basis functions do satisfy the correct asymptotic boundary conditions and the calculated cross sections are Galilean invariant. However, these *ad hoc* ETF's are semiclassical in nature, even though the same formulation has been applied to quantum mechanical formulations as well [15,14].

In spite of these limitations, a large number of calculations based on the MO-ETF models have been carried out for low-energy ion-atom collisions, and the results often compare reasonably well with experiments. On the other hand, ion-atom collision experiments at low energies are very difficult and experiments often can determine total charge-transfer cross sections only. Thus the validity of the MO-ETF-type calculations has not been fully tested at the high-precision level. In this paper we present a theoretical approach for ion-atom collisions at low energies. Our goal is to provide results for elementary ion-atom collision systems so that they can be used to evaluate the validity of other

methods such as the MO-ETF-type models. As a numerical implementation of this theory, charge transfer cross sections in $He^{2+}+H$ collisions are presented.

The simplest ion-atom collision system consists of two heavy nuclei and one electron. They belong to a special class of Coulomb three-body systems. In recent decades, the hyperspherical close-coupling (HSCC) approach has been shown to provide a powerful framework for obtaining structure parameters and scattering cross sections involving three particles [19]. The method has been used to study helium atoms [20], positron-atom collisions [21] (two light particles and one heavy), atom-diatom collisions [22,23], muonic molecules [24], and three-body recombinations [25] (three particles of identical or nearly identical masses). It was emphasized earlier by Fano and co-workers [26] that the fundamental difficulties of the PSS model can be avoided if one formulates ion-atom collisions within the hyperspherical framework. However, few actual calculations have been done. For ion-atom collisions, even at thermal energies, the number of partial waves needed to reach a converged total cross section calculation easily runs into hundreds or thousands. In the standard HSCC method, unlike the PSS approach, each partial wave is an independent calculation; thus the hyperspherical approach would require huge computational resources. However, it has been shown recently by Igarashi and Lin [27] that simplifications similar to those of the PSS model can be applied to ion-atom collisions within the hyperspherical approach. Using a simple two-channel model, charge transfer cross sections in $D^+ + H(1s)$ collisions [27] and in $\mu^+ + H(1s)$ collisions [28] have been obtained, but only for energies up to a few eV. To generalize these earlier studies to many-channel problems and to take advantage of simplifications similar to the PSS model, as detailed below, the hyperspherical approach has to be formulated in the body frame of the three-body system, and a number of numerical difficulties have to be overcome if it is to be extended to the tens of keV region.

In this paper we present a full account of the hyperspherical close-coupling method for ion-atom collisions. The formulation is similar to the PSS model except that the hyperradius is used as the adiabatic parameter. Computationally, we adopted the following techniques. First, the total wave function is expanded in the body-fixed frame, with the internuclear axis chosen to be the body-frame quantization axis. The adiabatic hyperspherical channel functions are calculated using *B*-spline basis functions. Second, the slow/smooth variable discretization (SVD) method [29], combined with the *R*-matrix propagation method of Kato and Watanabe [30], is used to solve the coupled hyperradial equations. The latter method allows us to avoid calculating nonadiabatic coupling matrix elements. Third, the *R* matrix from the inner region and the asymptotic solutions are matched at a large hyperradius to obtain the *K* matrix and then the scattering cross sections. Simplifications and modifications of the procedures used by Kato and Watanabe [30] needed for ion-atom collision systems are also explained.

For a pilot calculation, we studied the charge transfer process in slow $He^{2+}+H(1s)$ collisions at center-of-mass energies from 10 eV to 4.0 keV. The results are compared with other calculations. At higher energies the present results are in general agreement with other calculations and experiments. However, we found significant discrepancy with the MO-ETF calculations [15] at low energies. In the low-energy region, our results are in good agreement with those obtained from the distorted atomic orbital method [31], despite the fact that the latter has never been fully developed into a practical computational tool because of its mathematical complexity. In Sec. II, we describe the hyperspherical close-coupling method. The details of the computational procedures and tests are described in Sec. III. In Sec. IV, we present our calculated charge-transfer cross sections for $He^{2+}+H(1s)$ collisions and compare them with other theoretical calculations. The last section gives a summary and conclusions.

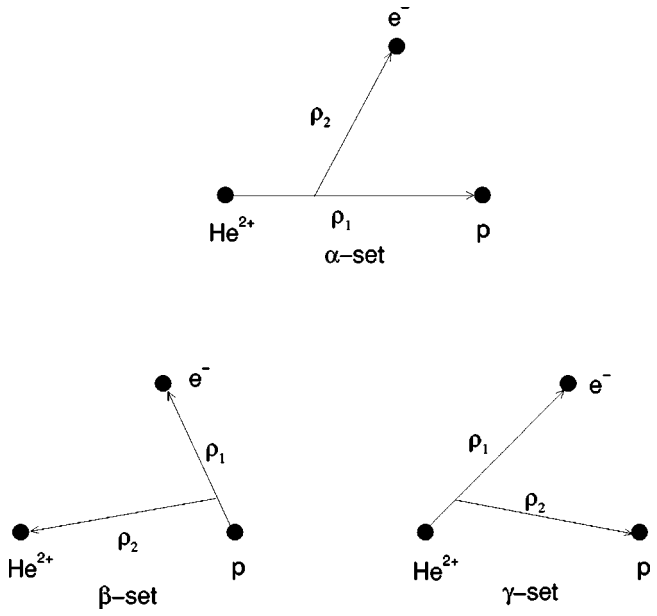

FIG. 1. Three sets of Jacobi coordinates.

II. HYPERSPHERICAL METHOD FOR ION-ATOM COLLISIONS

In this section we describe the theoretical methods and the computational techniques used in the hyperspherical method for treating ion-atom collisions. A detailed description of hyperspherical coordinates for arbitrary three-body systems is given in the review by Lin [19]. Here we give only the basic equations and the computational methods used in the present work.

A. Elements of the hyperspherical close-coupling method

For collisions such as $He^{2+}+H$, we describe the collision process in the center-of-mass frame. Using atomic units, we designate the mass of each of the three particles by m_1, m_2, and m_3, respectively. Three sets of Jacobi coordinates can be used to describe the relative motion of the particles (see Fig. 1). In the ''molecular'' frame, or the α set of coordinates, the first Jacobi vector $\boldsymbol{\rho}_1$ is from He^{2+} to H^+, with reduced mass μ_1; and the second Jacobi vector $\boldsymbol{\rho}_2$ is from the center of

mass of He^{2+} and H^+ to the electron, with reduced mass μ_2. The hyperradius R and hyperangle ϕ are defined by

$$R=\sqrt{\frac{\mu_1}{\mu}\rho_1^2+\frac{\mu_2}{\mu}\rho_2^2}, \tag{1}$$

$$\tan\phi=\sqrt{\frac{\mu_2}{\mu_1}}\frac{\rho_2}{\rho_1}. \tag{2}$$

Note that μ is arbitrary. Another angle θ, defined to be the angle between the two Jacobi vectors, will also be used later. The range of ϕ is from 0 to $\pi/2$ and θ ranges from 0 to π. Clearly, one can also define the two other sets of coordinates in Fig. 1. In the β-set coordinates, the first Jacobi vector is from He^{2+} to the electron, and the second Jacobi vector is from the center of mass of (He^{2+},e^-) to H^+. This set is used to describe the scattering of the proton with the bound He^+ ion. Similar γ-set Jacobi coordinates can be defined to describe He^{2+} and the (H^+,e^-) system. For each Jacobi coordinate system, a set of new mass-weighted hyperspherical coordinates similar to Eqs. (1) and (2) can be defined. A special notable feature is that the hyperradius thus defined is identical for the three sets of Jacobi coordinates. In the following we will express the equations using the α set of coordinates. When quantities are expressed in β- or γ-set coordinates, superscripts of β or γ will be used. In the α-set coordinates the formulation of the hyperspherical close-coupling method is very similar to the PSS model. We will choose μ to be the reduced mass of the two heavy nuclei. The hyperradius R then becomes very close to the internuclear distance. From Eq. (1), the difference is of the order of $\sqrt{\mu_2/\mu_1}$, which is roughly the square root of the mass of the electron over the reduced mass of the two heavy particles.

We first introduce the rescaled wave function

$$\Psi(R,\Omega,\hat{\omega})=\psi R^{3/2}\sin\phi\cos\phi; \tag{3}$$

then the Schödinger equation is of the form

$$\left(-\frac{1}{2}\frac{\partial}{\partial R}R^2\frac{\partial}{\partial R}+\frac{15}{8}+H_{\rm ad}(R;\Omega)-\mu R^2E\right)\Psi(R,\Omega,\hat{\omega})=0, \tag{4}$$

where $\Omega\equiv\{\phi,\theta\}$, and $\hat{\omega}$ denotes the three Euler angles $\{\omega_1,\omega_2,\omega_3\}$ of the body-frame axes with respect to the space-fixed frame. $H_{\rm ad}$ is the adiabatic Hamiltonian,

$$H_{\rm ad}(R;\Omega,\hat{\omega})=\frac{\Lambda^2}{2}+\mu RC(\Omega), \tag{5}$$

where Λ^2 is the square of the grand angular momentum operator and C/R is the total Coulomb interaction among the three charges. Equation (4) can be solved in a manner similar to the Born-Oppenheimer approximation with R being treated as a slow variable.

We solved the wave function in the body frame, where the z' axis is chosen to be along $\boldsymbol{\rho}_1$ and the three particles are on the $x'z'$ plane. The rescaled wave function is expanded in terms of the normalized and symmetrized rotation functions $\tilde{D}$ [32] and the body-frame adiabatic basis functions $\Phi_{\mu I}(R;\Omega)$:

$$\Psi(R,\Omega,\hat{\omega})=\sum_{\mu}\sum_{I}F_{\mu I}(R)\Phi_{\mu I}(R;\Omega)\tilde{D}^J_{IM_J}(\omega_1,\omega_2,\omega_3), \tag{6}$$

where μ is the channel index, J is the total angular momentum, I is the absolute value of the projection of **J** along the z' axis, and M_J is the projection of **J** along the space-fixed z axis.

In the body frame, the Λ^2 operator takes the form

$$\Lambda^2=T_0+T_1+T_2-1/4, \tag{7}$$

where

$$T_0=-\frac{\partial^2}{\partial\phi^2}-\frac{1}{\sin^2\phi\cos^2\phi\sin\theta}\frac{\partial}{\partial\theta}\left(\sin\theta\frac{\partial}{\partial\theta}\right), \tag{8}$$

$$(\tilde{D}^J_{IM_J}|T_1|\tilde{D}^J_{I'M_J})=\left[I^2\left(\frac{1}{\sin^2\phi\cos^2\phi\sin^2\theta}-\frac{2}{\cos^2\phi}\right)+J(J+1)\left(\frac{1}{\cos^2\phi}\right)\right]\delta_{II'}, \tag{9}$$

$$(\tilde{D}^J_{IM_J}|T_2|\tilde{D}^J_{I'M_J})=\gamma^J_{II+1}h_{II+1}\delta_{I'I+1}+\gamma^J_{II-1}h_{II-1}\delta_{I'I-1}=\overline{T_2}, \tag{10}$$

with

$$h_{II\pm1}=\frac{1}{\cos^2\phi}\left(\pm\frac{\partial}{\partial\theta}+(I\pm1)\cot\theta\right), \tag{11}$$

$$\gamma^J_{II+1}=-[1+(\sqrt{2}-1)\delta_{I0}][(J+I+1)(J-I)]^{1/2}, \tag{12}$$

$$\gamma^J_{II-1}=-[1+(\sqrt{2}-1)\delta_{I0}][(J-I+1)(J+I)]^{1/2}. \tag{13}$$

Note that the brackets $(||)$ denote an integration over $\hat{\omega}$. Only T_2 couples the internal motion to the external rotation. While both matrix elements of T_0 and T_1 are diagonal in I, T_2 couples adjacent I's.

In order to efficiently treat a large number of partial waves, Λ^2 is separated into two parts, each of which depends only on I and J, respectively,

$$(\tilde{D}^J_{IM_J}|T_1|\tilde{D}^J_{IM_J})=I^2T_{1a}+J(J+1)T_{1b}. \tag{14}$$

The adiabatic basis functions $\Phi_{\mu I}(R;\Omega)$ are chosen to satisfy

$$[T_0+I^2T_{1a}+2\mu CR]\Phi_{\mu I}(R;\Omega)=2\mu R^2U^I_\mu(R)\Phi_{\mu I}(R;\Omega). \tag{15}$$

The $\Phi_{\mu I}$ are obtained by solving the eigenvalue problem with a large two-dimensional (θ and ϕ)B-spline basis set [33], thus determining adiabatic potential curves $U^I_\mu(R)$ for

each I and a set of orthonormal adiabatic basis functions $\Phi_{\mu I}(R;\phi,\theta)$ that depend parametrically on R. Specifically, the channel functions are expanded onto a direct product of fifth-order B splines in ϕ and θ; the details are described in the next section. Note that $\Phi_{\mu I}$ is not an eigenfunction of the adiabatic Hamiltonian $H_{\rm ad}$ in Eq. (5). The eigenfunctions of the adiabatic Hamiltonian can be obtained by diagonalizing the tridiagonal block matrix constructed by

$$\begin{pmatrix} A^{I=0} & B^{+} & \cdots \\ B^{-} & A^{I=1} & \cdots \\ \vdots & \vdots & \ddots \end{pmatrix}, \tag{16}$$

where

$$A^{I}_{\mu\nu}(R)=2\mu R^2 U^{I}_{\mu}\delta_{\mu\nu}+J(J+1)\langle\Phi_{\mu I}|T_{1b}|\Phi_{\nu I}\rangle, \tag{17}$$

$$B^{\pm}(R)=\langle\Phi_{\mu I}|\overline{T}_2|\Phi_{\nu I\pm1}\rangle=\gamma^{J}_{II\pm1}\langle\Phi_{\mu I}|h_{II\pm1}|\Phi_{\nu I\pm1}\rangle. \tag{18}$$

Note that the brackets $\langle||\rangle$ denote integration over Ω.

The advantage of this partition is that these basis functions Φ need to be calculated only once for all the J's. So do the matrix elements $\langle\Phi_{\mu I}|T_{1b}|\Phi_{\nu I}\rangle$ and $\langle\Phi_{\mu I}|h_{II\pm1}|\Phi_{\nu I\pm1}\rangle$, which are required in constructing matrices A and B. As a result, constructing the adiabatic Hamiltonian for a given J involves only fast algebraic operations within a given I subspace. Such an efficient approach is critical since hundreds or thousands of partial waves need to be included in order to obtain a converged cross section even for collisions at thermal energies and above.

B. *R*-matrix propagation with SVD method

The standard method of solving the Schrödinger equation [cf. Eq. (4)] with the expansion of Eq. (6) is to project out the adiabatic basis functions, resulting in a set of coupled differential equations for the hyperradial functions $F_{\mu I}$. It is well known that such coupled differential equations are difficult to solve accurately since the coupling matrix elements change rapidly in the avoided crossing regions. Two well-known procedures have been used to address such numerical difficulties. The first is the ''diabatization'' of the subset of adiabatic functions, commonly employed in ion-atom and ion-molecule collision calculations within the PSS or MO-ETF model [14,34–36]. Before the diabatization procedure, one needs to obtain nonadiabatic coupling matrix elements accurately, and this has to be done very carefully in the region of an avoided crossing. The second method, which was designed to bypass the calculation of nonadiabatic coupling matrix elements, is the so-called diabatic-by-sector method [20,37]. This method was used in earlier hyperspherical close-coupling calculations and in atom-diatom reactive scattering calculations [22,23,38]. In this approach, the hyperradius is divided into many small sectors and within each sector the channel functions are fixed and chosen to be the adiabatic channel functions at the midpoint within the sector. The diabatic-by-sector method simplifies the calculation but the method in principle is not mathematically complete even if the sector size is reduced to zero [39]. In practice, this means slower convergence in the calculation.

Here we adopt yet another efficient method to solve the hyperradial equations. It is a combination of the R-matrix propagation method [40], which propagates the R matrix from one sector to the next, and the SVD method [29] within each sector, where the Hamiltonian is a smoothly varying function of R. This method was adopted by Kato and Watanabe [30] for solving the two-electron atomic Schrödinger equation and by Tolstikhin and Nakamura [41] for atom-diatom collisions. The key elements of the method and modifications that are needed for the present ion-atom collision problems are presented below.

The R-matrix propagation method is a stable and efficient way to solve a set of coupled differential equations [40]. In this approach, the hyperradius is divided into many small finite intervals. Solutions within each interval are calculated and propagated with respect to the hyperradius.

We start with the Schrödinger equation, Eq. (4). Solutions within an interval $[a,b]$ can be formally written in terms of the Green's function defined within the interval

$$\Psi(R,\Omega)=\int_a^b dR'\int d\Omega'\,\mathcal{G}(R,\Omega;R',\Omega')\mathcal{L}(R')\Psi(R',\Omega'), \tag{19}$$

where $\mathcal{L}$ is the Bloch operator defined as

$$\mathcal{L}(R)=R^2\left[\delta(R-b)\frac{\partial}{\partial R}-\delta(R-a)\frac{\partial}{\partial R}\right]. \tag{20}$$

A spectral resolution of the Green's function can be written as

$$\mathcal{G}(R,\Omega;R',\Omega')=\sum_k\frac{u_k(R,\Omega)u_k(R',\Omega')}{\mu(E_k-E)}, \tag{21}$$

where $\{u_k(R,\Omega),E_k\}$ are the solutions of the eigenvalue problem

$$\left[-\frac{1}{2}\frac{\partial}{\partial R}R^2\frac{\partial}{\partial R}+\frac{15}{8}+H_{\rm ad}(R;\Omega)+\mathcal{L}-R^2\mu E_k\right]u_k(R,\Omega)=0. \tag{22}$$

This equation is to be solved using the SVD method developed by Tolstikhin *et al.* [29]. The method treats the Schrödinger equation in the discrete-variable representation (DVR) [42] with respect to R. A set of DVR basis functions are constructed using orthonormal basis functions based on Jacobi polynomials of degrees up to $M-1$ within the interval $[a,b]$. The solution u_k then is expanded in terms of pointwise DVR basis functions $\pi_j(R)$ within an M-dimensional subspace,

$$u_k(R,\Omega)=\sum_{j=1}^{M}\pi_j(R)\Theta_{jk}(\Omega). \tag{23}$$

Note that DVR basis functions have the important property that $\pi_j(R_{j'})=\kappa_j^{-1}\delta_{jj'}$, where κ is a weight constant depending on the indices of the Jacobi polynomials. Then, Eq. (22) is transformed into a set of coupled differential equations with respect to the coefficients $\Theta_{jk}(\Omega)$,

$$H_{\rm ad}(R_j,\Omega)\Theta_{jk}(\Omega)+\sum_{j'=1}^{M}[K_{jj'}-\rho_{jj'}\mu E_k]\Theta_{j'k}(\Omega)=0, \tag{24}$$

where

$$K_{jj'}=\int_a^b \pi_j(R)\left(-\frac{1}{2}\frac{\partial}{\partial R}R^2\frac{\partial}{\partial R}+\frac{15}{8}+\mathcal{L}(R)\right)\pi_{j'}(R)dR, \tag{25}$$

$$\rho_{jj'}=\int_a^b \pi_j(R)R^2\pi_{j'}(R)dR. \tag{26}$$

These coefficients can be expanded in terms of the adiabatic channel functions Φ_n,

$$\Theta_{jk}(\Omega)=\sum_n \Phi_n(R_j,\Omega)c_{njk}, \tag{27}$$

where $n=\{\mu I\}$ and the R_j's are the quadrature abscissas of the Jacobi polynomial of degree M within the interval $[a,b]$. The set of coupled differential equations (24) is then transformed into an algebraic generalized eigenvalue problem,

$$\sum_{n'}\left[\overline{U}_{nn'}(R_j)c_{n'jk}+\sum_{j'=1}^{M}[K_{jj'}-\rho_{jj'}\mu E_k]O_{nj,n'j'}c_{n'j'k}\right]=0, \tag{28}$$

where

$$\overline{U}_{nn'}(R_j)=\langle\Phi_n(R_j)|H_{\rm ad}|\Phi_{n'}(R_j)\rangle, \tag{29}$$

$$O_{nj,n'j'}=\langle\Phi_n(R_j)|\Phi_{n'}(R_{j'})\rangle. \tag{30}$$

The M-point Gauss quadrature is used to evaluate the integration over R in Eqs. (28), (29), and (30). Therefore, we need to solve the eigenvalue problem Eq. (15) only at the values of R corresponding to the quadrature abscissas of the Jacobi polynomials of degree M within each interval.

Using the SVD method, there is no need to calculate nonadiabatic coupling matrix elements; their effects are implicitly incorporated by the overlap matrix elements of the adiabatic channels at different hyperradii R. Note that the calculation of the overlap matrix elements at different values of the hyperradius is time consuming. However, these overlapping matrix elements need to be calculated only once, since the adiabatic channels [cf. Eq. (15)] are independent of the total angular momentum J.

Once the basis functions u_k are obtained, the solution $\Psi(R,\Omega)$ can be readily constructed:

$$\Psi(R,\Omega)=\sum_k \frac{u_k(R,\Omega)}{\mu(E_k-E)}\left[b^2\left\langle u_k\left|\frac{\partial\Psi}{\partial R}\right\rangle_{R=b}-a^2\left\langle u_k\left|\frac{\partial\Psi}{\partial R}\right\rangle_{R=a}\right.\right]. \tag{31}$$

The $\mathcal{R}$ matrix with respect to the adiabatic channels is defined at the boundaries of the interval as

$$\langle\Phi_n|\Psi\rangle=\sum_m \mathcal{R}_{nm}(R)\left\langle\Phi_m\left|\frac{\partial\Psi}{\partial R}\right\rangle\right. . \tag{32}$$

The propagation formula for the $\mathcal{R}$ matrix is in the form

$$\mathcal{R}_{nm}(b)=G_{nm}^{bb}-\sum_l\sum_{l'}G_{nl}^{ba}[G^{aa}+\mathcal{R}(a)]^{-1}_{ll'}G_{l'm}^{ab}, \tag{33}$$

where

$$G_{nm}^{R_1R_2}=R_1R_2\sum_k\frac{\langle\Phi_n(R_1)|u_k(R_1)\rangle\langle u_k(R_2)|\Phi_m(R_2)\rangle}{\mu(E_k-E)}. \tag{34}$$

The $\mathcal{R}$ matrix is set to zero at $R=0$. Solutions are calculated and propagated to large R in order to obtain the $\mathcal{R}$ matrix at an asymptotic hyperradius, where the hyperspherical channels converge to various atomic target states and $F_{\mu I}$ can be matched to asymptotic solutions. The advantage of the R-matrix propagation is its stability. Unlike the wave function itself, there are no exponentially decreasing or increasing functions in the propagation. Also, the basis functions used in constructing the propagators are energy independent, making it efficient to obtain wave functions for different energies. Further details of the methods can be found in Refs. [29,30].

C. Matching to the asymptotic solutions

The R-matrix propagation method can be continued up to a large hyperspherical radius R_0 beyond which one particle is far away from the other pair of particles. In this work we do not consider the three-body breakup process; thus the asymptotic wave function $\Psi_\lambda^{\rm as}(R_0)$ of the dissociated system is represented by

$$\Psi_\lambda^{\rm as}(\boldsymbol{\rho}_1,\boldsymbol{\rho}_2)=\sum_{i=1}^{N}[f_i(k_{i\tau}\rho_2^\tau)\delta_{i\lambda}-g_i(k_{i\tau}\rho_2^\tau)K_{i\lambda}]\varphi_i(\rho_1^\tau)\mathcal{Y}_{l_1^\tau l_2^\tau JM_J}(\hat{\boldsymbol{\rho}}_1^\tau,\hat{\boldsymbol{\rho}}_2^\tau)/\rho_1^\tau\rho_2^\tau, \tag{35}$$

where the wave function is expressed in the laboratory-fixed frame and the base functions are given in $\tau=\beta$- or γ-set coordinates. For the present Coulomb three-body system, φ_i is a hydrogenic radial wavefunction with angular momentum l_1, and the relative angular momentum between the hydrogenlike atom and the heavy particle is l_2, coupled to form a total angular momentum function $\mathcal{Y}_{l_1l_2JM_J}$, with total angular

momentum J and its projection with respect to the laboratory fixed quantization axis, M_J. f and g are the regular and irregular asymptotic functions. For the $He^{2+}+H$ asymptotic limit, they are Bessel functions and Neumann functions, respectively. For the $H^+ + He^+$ asymptotic limit, they are regular and irregular Coulomb functions, respectively. Note that the wave vector k depends on the Jacobi coordinates used. They are related to the kinetic energy for each channel by

$$\frac{1}{2\mu_1^\alpha}k_\alpha^2=\frac{1}{2\mu_2^\beta}k_\beta^2=\frac{1}{2\mu_2^\gamma}k_\gamma^2=E-U_\nu(\infty). \tag{36}$$

The general asymptotic solution (35) is matched to the inner solution obtained from the R-matrix propagation,

$$\frac{1}{R_0^{5/2}\sin\phi\cos\phi}\sum_{\sigma=1}^{N} H_{\sigma\lambda}\Psi^\sigma(R_0)=\Psi_\lambda^{\rm as}(\boldsymbol{\rho}_1,\boldsymbol{\rho}_2)\big|_{R=R_0}, \tag{37}$$

where the inner solution is expressed in α-set coordinates and the matching is to be carried out at $R=R_0$. Such a matching procedure was discussed and employed by Zhou and Lin [21] for $e^+ + H(1s)$ collisions previously. It involves transforming the β- and γ-set wave functions into the α-set coordinates, from where integration over all the angular coordinates at $R=R_0$ is carried out. In practice, this requires a two-dimensional numerical integration involving (ϕ,θ) and the procedure is called two-dimensional matching. From the resulting K matrix, the partial cross sections are obtained:

$$\sigma_{ij}=\frac{4\pi(2J+1)}{k_i^2}\left|\frac{\mathbf{K}}{1-i\mathbf{K}}\right|_{ij}^2. \tag{38}$$

Since the wave functions beyond R_0 are represented in either the β- or γ-set Jacobi coordinates depending on the dissociation channels, there is no spurious coupling between the channels.

Calculation of the K matrix using the two-dimensional matching method is often used for calculations at higher precision and at low collision energies. For ion-atom collisions where the matching has to be carried out for each partial wave, it is desirable to simplify the calculation. Consider the Bessel and Coulomb functions, which are written as $f(k_\tau\rho_2^\tau)$ and $g(k_\tau\rho_2^\tau)$ in Eq. (35); the argument has been written in terms of Jacobi coordinates. Let the masses of each of the three particles be m_1, m_2, and 1.0, where the last is the mass of the electron. The hyperspherical radius is related to ρ_1 and ρ_2 for each Jacobi set τ by

$$\begin{aligned}R&=\sqrt{\frac{\mu_1^\alpha}{\mu}}\sqrt{\rho_{1\alpha}^2+\frac{\mu_2^\alpha}{\mu_1^\alpha}\rho_{2\alpha}^2}=\sqrt{\frac{\mu_2^\beta}{\mu}}\sqrt{\rho_{2\beta}^2+\frac{\mu_1^\beta}{\mu_2^\beta}\rho_{1\beta}^2}\\&=\sqrt{\frac{\mu_2^\gamma}{\mu}}\sqrt{\rho_{2\gamma}^2+\frac{\mu_1^\gamma}{\mu_2^\gamma}\rho_{1\gamma}^2}.\end{aligned} \tag{39}$$

At the matching radius R_0, ρ_1 is of the same order as ρ_2 for the α set, but ρ_2 is much larger than ρ_1 for the two other sets. Since the ratios of the reduced masses within the square roots of Eq. (39) are all roughly equal to the ratio of the mass of the electron to the mass of the heavy particle for any set of Jacobi coordinates, at R_0 we can approximate

$$R_0=\sqrt{\frac{\mu_1^\alpha}{\mu}}\rho_{1\alpha}=\sqrt{\frac{\mu_2^\beta}{\mu}}\rho_{2\beta}=\sqrt{\frac{\mu_2^\gamma}{\mu}}\rho_{2\gamma}. \tag{40}$$

By setting $\mu=\mu_1^\alpha$, the argument of the Bessel and/or Coulomb function in the β-set coordinates, $k_\beta\rho_2^\beta$, from Eqs. (36) and (40), is equal to $k_\alpha R_0$. The same is true for the argument in the γ-set coordinates. In other words, the argument in the Bessel and/or Coulomb functions for each channel calculated from the α-set coordinates does agree with the argument calculated in the β-set and γ-set coordinates. Since the adiabatic energies calculated in hyperspherical coordinates do approach the correct asymptotic energies in the dissociation limit, at least to order of $1/R^2$ [43], it is possible to skip the two-dimensional matching all together, and obtain the K matrix directly within the α-set coordinates. This is called one-dimensional matching. We have tested our calculations using one-dimensional and two-dimensional matching methods, by changing the matching radius, and concluded that one-dimensional matching is adequate in general except at very low energies.

For the present $He^{2+}+H$ collision system, there is one additional complication which we need to address. For the charge transfer to $He^+(2s)$ or $He^+(2p)$ states, the asymptotic limits are degenerate. The adiabatic channel functions from the inside region are correlated with the dipole states [44,45] with noninteger or even complex angular momentum for each partial wave J. We do not consider this complication in the matching procedure in the present work. However, we established that the J-dependent charge transfer cross sections to $2s$ plus $2p$ states thus obtained are not dependent on the matching radius. Thus we do not consider charge-transfer cross sections to individual $2s$ or $2p$ states in this work. We comment that cross sections to such individual degenerate hydrogenic final states can be calculated directly using the two-dimensional matching procedure, or in a one-dimensional matching procedure if dipole states are used instead of Coulomb functions [44,45].

III. NUMERICAL DETAILS

In applying the hyperspherical close-coupling method to ion-atom collisions, special care is needed in two areas in the numerical implementation. We used B-spline basis functions to obtain adiabatic channel functions, but the choice of the grid distributions has to be tailored to the nature of the channel functions that are concentrated in the region of small ϕ. This is clearly seen from Eq. (2), which shows that the range of ϕ is of the order of the square root of the mass of the electron with respect to the mass of the nuclei. Furthermore, attractive Coulomb singularities occur at small ϕ's, at $\phi_1=5.25\times10^{-3}$ and $\phi_2=2.08\times10^{-2}$ rad, respectively, for the present $He^{2+}+H$ system. The ϕ grids were chosen such that they are concentrated in the small-ϕ region. Specifically, we divided $\phi=[0,\pi/2]$ into four intervals, with N_1 points in $[0,\phi_1]$, N_2 points in $[\phi_1,(\phi_1+\phi_2)/2]$, N_3 points in

$[(\phi_1+\phi_2)/2,\phi_2]$, and N_4 points in $[\phi_2,\pi/2]$. Within each interval $[\phi_a,\phi_b]$, an exponential sequence of grid points is chosen according to

$$\phi_i=\phi_a+(\phi_b-\phi_a)\frac{e^{\gamma(i-1)}-1}{e^{\gamma(N-1)}-1} \tag{41}$$

for $i=1,\ldots,N$. In the present calculation we chose $\gamma=0.3$, $N_1=14$, $N_2=N_3=16$, and $N_4=34$ such that there are 80 points in ϕ. Only ten points were used for the interval $\phi=[0.1,\pi/2]$ in this grid distribution. For the θ grids, we used 61 points in the range $[0,\pi]$. The grids are distributed symmetrically about $\theta=\pi/2$, in an exponential sequence according to Eq. (41), with $\gamma=0.075$. The parameters in the grid distributions were varied to reach at least six-digit accuracy in the eigenvalues for the range of R of interest. Different grid distributions can be used in different ranges of R in the method, but in the present calculation this particular set of grid points was used in the final calculation.

In the SVD method the channel functions are to be calculated at the hyperradial points dictated by the grid distributions chosen for the R-matrix propagation, following the procedure of Sec. II B. Thus the range $[0,R_0]$ is divided into many intervals. Within each interval, the hyperradial grid points are determined by the order M of the Jacobi polynomials used in the DVR representation of the hyperradial functions. Ideally one would like to have about ten points per wavelength in the hyperradial function. Such a prescription was used by Kato and Watanabe [30], who applied this method to electron-atom collisions. A straightforward application of their procedure to ion-atom collisions is not practical. Due to the large reduced mass, the momentum that enters Eq. (4), as given by $\sqrt{2\mu(E-U)}$, becomes quite large even at thermal energies. For example, for the present $He^{2+}+H$ system at center-of-mass energy of, say, 500 eV, we would need about 10 000 points within the interval of $R=[0,40]$ if we wish to have about ten points per wavelength in the hyperradial function. Since the calculation of the channel function is the most time-consuming part, this is clearly not desirable. On the other hand, while the radial wave functions oscillate rapidly, all the matrix elements entering the SVD method are slow-varying functions of the hyperradius. Thus, instead of calculating all the matrices needed in the SVD method, we obtained these matrix elements by interpolation.

Specifically, instead of calculating the matrix elements

$$\langle\Phi_{\mu I}(R_i;\theta,\phi)|T_{1b}|\Phi_{\nu I}(R_i;\theta,\phi)\rangle,$$

$$\langle\Phi_{\mu I}(R_i;\theta,\phi)|h_{II\pm1}|\Phi_{\nu I\pm1}(R_i;\theta,\phi)\rangle,$$

and the overlaps $\langle\Phi_{\mu I}(R_i;\theta,\phi)|\Phi_{\nu I}(R_j;\theta,\phi)\rangle$ at all hyperradial grid points required for SVD and R-matrix propagation, we calculated them at a much smaller number of points and then use interpolations to obtain the required matrix elements. In practice, we used cubic (bicubic for two-dimensional interpolation of the overlaps) splines. In the present calculation we chose to interpolate only in the region where the overlaps, as functions of the hyperradius, are smooth, although in principle one can interpolate near the avoided crossing region as well if more points are initially calculated in the region.

TABLE I. Comparison of the partial wave charge transfer cross sections (in a.u.) obtained by using exact and interpolated matrix elements. The number in square brackets denotes the power of 10. See the text for more detail.

J		$E_{\text{c.m.}}=210$ eV capture cross section	$E_{\text{c.m.}}=510$ eV capture cross section
1	"exact"	0.25213[−4]	0.10101[−3]
	interp1	0.25213[−4]	0.10101[−3]
	interp2	0.24324[−4]	0.11399[−3]
10	"exact"	0.15530[−2]	0.11910[−2]
	interp1	0.15530[−2]	0.11910[−2]
	interp2	0.15368[−2]	0.11896[−2]
100	"exact"	0.35516[−2]	0.72555[−2]
	interp1	0.35516[−2]	0.72548[−2]
	interp2	0.35484[−2]	0.71972[−2]
500	"exact"	0.17987[−3]	0.32464[−3]
	interp1	0.17986[−3]	0.32465[−3]
	interp2	0.17693[−3]	0.32129[−3]
1000	"exact"	0.96640[−4]	0.21897[−2]
	interp1	0.96640[−4]	0.21896[−2]
	interp2	0.93522[−4]	0.21724[−2]
2000	"exact"	0.22715[−6]	0.80453[−3]
	interp1	0.22717[−6]	0.80452[−3]
	interp2	0.25344[−6]	0.80061[−3]

In Table I we compare partial wave cross sections (J dependence) for charge transfer into the $He^+(n=2)$ states ob-

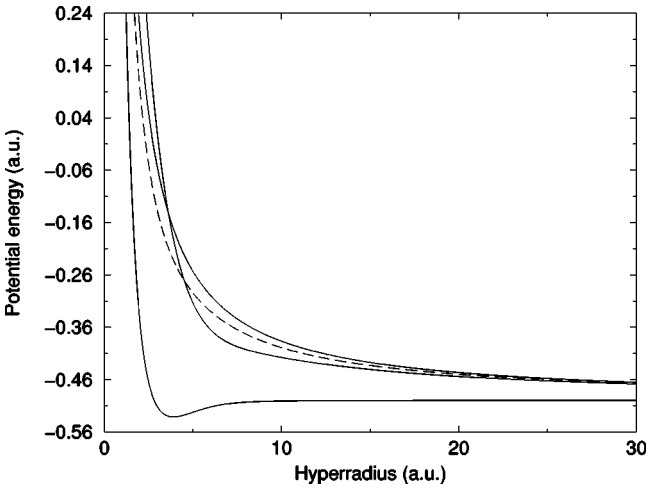

FIG. 2. Hyperspherical potential curves U_μ^I [cf. Eq. (15)] for HeH^{2+}. Three $I=0$ channels and one $I=1$ channel are shown by solid and dashed lines, respectively.

tained with the interpolation procedure at center-of-mass energies of 210 and 510 eV. All the calculations were carried out using the four channels shown in Fig. 2 and the propagation in R was carried out from $R=0$ to $R=32.32$ a.u. In the ''exact'' calculation we employed the straightforward SVD method within each sector where all the relevant matrix elements were calculated directly from the adiabatic channel functions. At 510 eV (210 eV) this would require us to calculate channel functions and all the relevant matrix elements at about 10 000 (6000) hyperradial grid points. For the two interpolation procedures, Interp1 and Interp2, we calculated adiabatic channel functions only at 2520 and 630 hyperradial grid points, respectively, from which we obtained the SVD matrix elements at the same grid points as in the ''exact'' calculation. In the present work, we did not perform interpolation in the interval $R=[0,0.5]$, where the channel functions vary rapidly with R, and the intervals $[1.5,2]$ and $[3.5,4]$, where they are near the avoided crossings at $R=1.65$ a.u. and 3.62 a.u., respectively. In these intervals we simply calculate channel functions at denser grid points.

In Table I, we note that the results from the Interp1 calculation are essentially identical to the ''exact'' calculations. The errors introduced in the Interp2 calculation are within 1% for most of the partial waves. In particular, the relative errors are smaller for partial waves where the cross sections are larger. We thus conclude that the interpolation procedure works adequately.

From Eqs. (14) and (17), the matrix elements of T_{1b}, or of $1/\cos^2\phi$, with respect to the adiabatic channel functions have to be evaluated. The channel functions are sharply localized near $\phi=0.0$, the more so at larger R. From Eq. (14), we note that we need to add $J(J+1)T_{1b}$ to obtain the matrix element T_1. For large J, in particular, for $J>10^3$, any small numerical error from T_{1b} is greatly enhanced in comparison with T_{1a}. For large J, we found that it is preferable to replace the matrix element of T_{1b} by 1.0 instead. In fact, this replacement does not affect the result for small J either. We note that this is the same approximation employed in the PSS calculation.

IV. RESULTS

In this paper we applied the HSCC method to calculate charge-transfer cross sections for $He^{2+}+H(1s)$ collisions at center-of-mass energies from 10 eV up to 4 keV, or for relative collision velocity v from 0.0223 a.u. to 0.447 a.u.. The dominant reaction channels are charge transfer to the $n=2$ excited states of He^+. Thus we include only four channels in the present calculation: the initial channel $He^{2+}+H(1s)$, and the three final channels $He^+(n=2)+H^+$. In Fig. 2 the four adiabatic hyperspherical potential curves corresponding to these four dissociation channels are shown: three curves for $I=0$ and one for $I=1$, for R up to 30 a.u. The incident channel is identified with the lowest curve of Fig. 2 and the three charge transfer channels are associated with the three upper curves.

The potential curves in Fig. 2 are very close to the BO potential curves in the standard PSS approach. This is not surprising since with the choice of $\mu=\mu_1$ [cf. Eq. (1)], the hyperradius R is approximately equal to the internuclear distance as long as R is not very small. But there are small differences. We found that, except for $R<1.5$ a.u., the differences between the hyperspherical potential curves and the BO potential curves are less than 1%. Also, the BO potential curves do not converge to correct thresholds, whereas the hyperspherical potentials do, although the energy difference at $R\to\infty$ is very small, about 3×10^{-4} a.u., owing to the fact that in the BO approximation the mass of the nucleus is assumed to be infinity, but in the HSCC the correct mass of the nucleus is included. In the present HSCC calculation, we used one-dimensional matching at $R_0=32.32$ a.u. for $E_{\mathrm{c.m.}}$ greater than 200 eV and $R_0=80.79$ a.u. at lower energies.

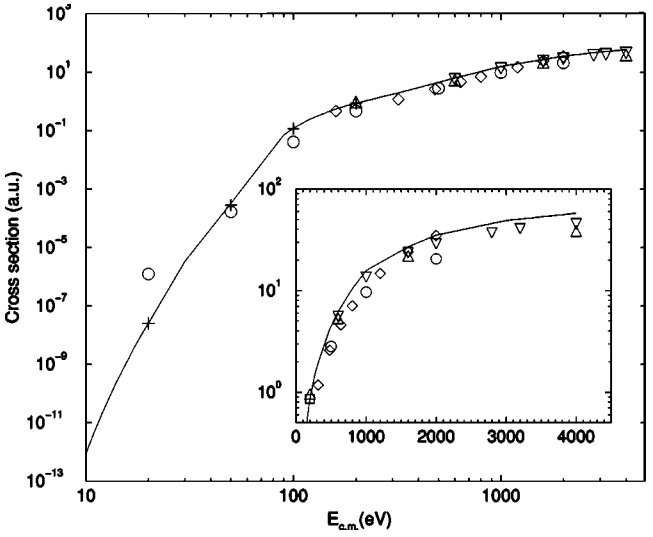

FIG. 3. Charge-transfer cross sections for the process $He^{2+}+H(1s)\to He^+ + p$. Solid line: present results; ○: van Hemert *et al.* [15]; +: Fukuda and Ishihara [31]; △: Winter and Hatton [49]; ▽: Errea *et al.* [50]; ◇: Grozdanov and Solov'ev [51].

In Fig. 3, total electron-transfer cross sections to He^+ states are presented from 10 eV to 4 keV. Note that the calculated charge-transfer cross section decreases rapidly as the collision energy is decreased. From 4 keV to 200 eV, it drops by a factor of 50 (see inset), but from 200 eV to 10 eV, it drops by 12 orders of magnitude. The small cross sections at the low energies are calculated to compare with other existing calculations. Note that at low energies radiative charge-transfer cross sections are much larger. The latter was calculated to be about 10^{-3} a.u. at $E=10$ eV [46]. Unlike that for the nonradiative process, the cross section for the radiative charge transfer increases with decreasing collision energy.

How do the results obtained here compare to existing experimental data and other calculations? For energies below 200 eV, there are no experimental data available. There are two previous theoretical calculations where the motion of the heavy particles was treated quantum mechanically. One was by van Hemert *et al.* [15] and the other by Fukuda and Ishihara [31]. The former performed calculations using molecular orbitals with common translational factor basis functions. From Fig. 3 it is clear that our results are significantly different from theirs below 200 eV. In fact, by comparing with the actual numbers, as shown in Table II, we note that their

TABLE II. Charge-transfer cross sections in units of 10^{-16} cm^2. The numbers in square brackets are powers of 10. WH: Winter and Hatton [49], CTF: Errea *et al.* [50], DMO-ETF: van Hemert *et al.* [15], DAO: Fukuda and Ishihara [31], HSCC: present results.

E(eV)	WH	CTF	DMO-ETF	DAO	HSCC
20			3.4[−7]	7.1[−9]	7.1[−9]
50			4.6[−5]	7.9[−5]	8.0[−5]
100			1.1[−2]	3.3[−2]	3.4[−2]
200	2.7[−1]		1.3[−1]	2.4[−1]	2.4[−1]
600	1.49	1.56			1.74
1000		3.78	2.69		4.42
1600	6.30	6.62			7.56
2000		8.07	5.73		9.86
4000	12.2	12.8			16.2

results are larger than ours by a factor of 50 at 20 eV, but theirs are smaller by a factor of 2, 3, and 2, respectively, at 50, 100, and 200 eV. Interestingly, in this energy region our results are in perfect agreement with the calculation of Fukuda and Ishihara [31]. They used the so-called distorted atomic orbital (DAO) method and carried out the calculation up to 200 eV. This method introduces adiabatic distorted atomic orbitals, defined not with respect to the internuclear separation, but with respect to the relative coordinates of each arrangement channel (or $\boldsymbol{\rho}_2$ of β-set and γ-set coordinates). In other words, they used basis functions from the β-set and from the γ-set coordinates. In the DAO method the wave function is expanded using correct relative coordinates such that there are no spurious asymptotic couplings. From Fig. 3, we note that their results agree with ours quite well. This agreement is even more clearly seen in Table II.

From comparing the three calculations in the low-energy region, we may conclude that the results of van Hemert *et al.* [15] are less reliable. At present, the origin of the difference is not clear. The cross sections are quite small in the low-energy region. The discrepancy could be due to the somewhat arbitrary character of the common electron translational factors used in their model, or possibly due to insufficient numerical accuracy in the calculation. Understanding the origin of this discrepancy is essential, however, since their MO-ETF approach is the most widely used method for treating low-energy ion-atom collisions [10,12,14]. On the other hand, to trace the origin of the discrepancy, a comparison at the level of partial wave cross sections should be carried out in the future. The comparison also appears to establish the validity of the DAO approach. Since two sets of Jacobi coordinates were used in this formulation, the result is a set of coupled integro-differential equations which can be solved only with special numerical techniques. The DAO method has been applied only to the present collision system and to muonic collisions [47] so far. It has not been further explored due to its numerical complications.

We next compare the present results with other calculations at higher energies where more calculations and some experimental data are available. The results for center-of-mass energy from 200 eV to 4 keV are shown more clearly in the inset of Fig. 3. The numerical values are also compared at a few energy points in Table II. Except for van Hemert *et al.* at 200 eV, all the other calculations were carried out using the semiclassical method where the internuclear motion is treated classically. All these calculations also used the molecular orbital expansion method [14,48,49,51]. The difference is mainly in the number of channels and the different form of electron translational factors used, except for Grozdanov and Solov'ev [51] where the calculation was based on the hidden crossing theory. From Fig. 3, we note that most of the theoretical results agree with each other. However, all of these other calculations essentially used the same method and agreement among themselves is not surprising. Comparing with available experimental data in this energy region, all the results are within the experimental errors. Our results appear to be slightly higher than these calculations. In the future we need to increase the number of channels in the higher-energy region to test the convergence of the present results.

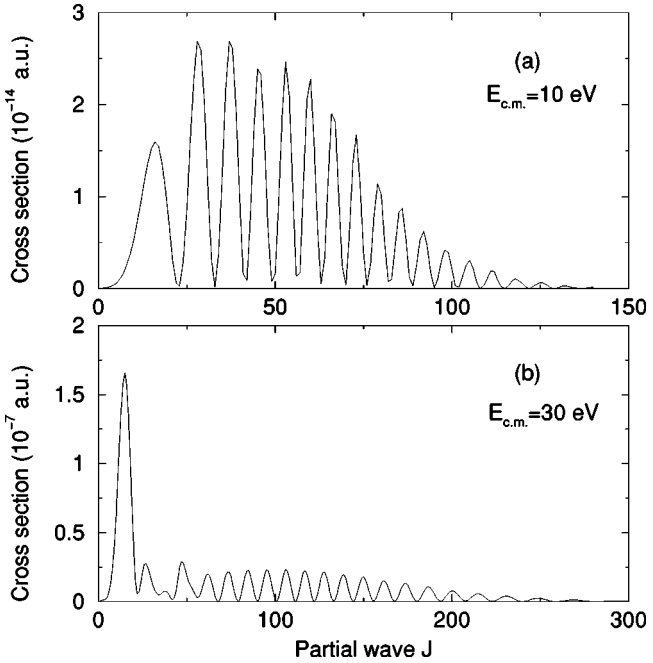

FIG. 4. Charge transfer partial cross section for $E_{\text{c.m.}}=10$ eV (a) and $E_{\text{c.m.}}=30$ eV (b).

We next show charge-transfer cross sections vs partial waves J at a few energy points. In Fig. 4(a), the results for $E=10$ eV are shown. It takes about 100 partial waves to get the converged total cross section. At 30 eV, as shown in Fig. 4(b), we need to sum over about 250 partial waves to get the total charge-transfer cross section, but a large portion of it is contributed by partial waves less than 20. Note the seven orders of magnitude difference in the partial cross sections at these two energies. In Fig. 5 we show our calculated partial wave cross sections for 200 eV and compare the results with those presented by Fukuda and Ishihara [31] for J between 150 and 950. Our results agree quite well with theirs, which in turn have been shown to agree well with the semiclassical calculation of Winter and Hatton [49]. Interestingly, these two groups did not present results at small partial waves or small impact parameters, even though the total charge-

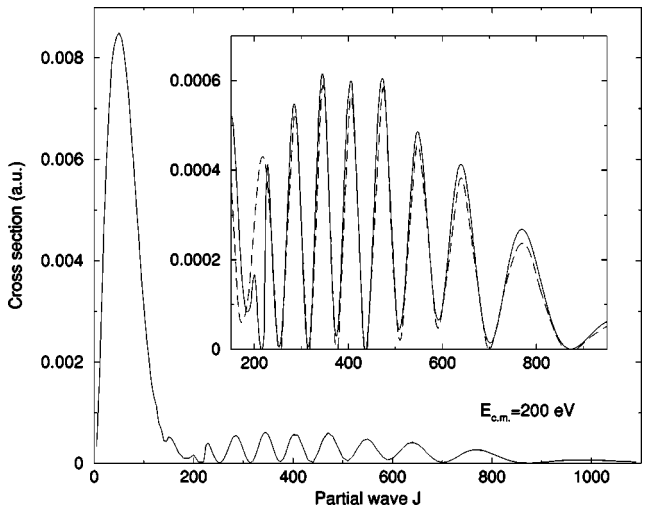

FIG. 5. Same as Fig. 4 but for $E_{\mathrm{c.m.}}=200$ eV. The dashed line in the inset is taken from Fukuda and Ishihara [31].

transfer cross section comes primarily from J less than 150. Since the total cross sections from these three calculations are in good agreement we assume that the partial cross sections at small J are also identical. In comparing the partial wave cross sections from the quantum calculation with the transition probabilities from the semiclassical calculation, we employ this relation:

$$\sigma_J=\frac{2\pi b P(b)}{k}, \tag{42}$$

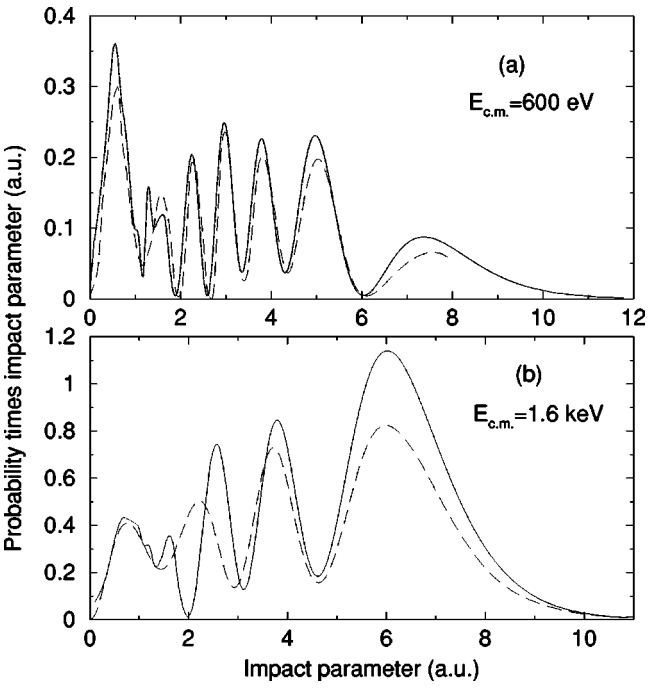

FIG. 6. Probability of charge transfer times impact parameter for $E_{\mathrm{c.m.}}=600$ eV (a) and $E_{\mathrm{c.m.}}=1.6$ keV (b). Solid lines: present results; dashed lines: Hatton *et al.* [48] and Winter and Hatton [49] for 600 eV and 1.6 keV, respectively.

with $J=kb$, where k is the momentum. In Fig. 6 we compare the impact parameter dependence of the calculated charge-transfer probabilities with those calculated by Hatton *et al.* [48] at 600 eV and by Winter and Hatton [49] at 1.6 keV. One can observe that there is a general agreement of our results with theirs, in terms of the impact parameters, where the weighted probabilities are at the maxima or minima, but our probabilities are somewhat higher at the peaks, resulting in our cross sections being somewhat higher compared to others. Since we used only four channels in the present calculation as compared to 10 channels in their calculations, the discrepancy can be better understood after we have performed calculations with a larger number of channels. The comparison illustrates that the present HSCC method can be extended to higher collision energies where semiclassical methods are valid.

V. SUMMARY AND CONCLUSIONS

In this paper we presented the hyperspherical close-coupling method for treating direct and charge-transfer reactions in ion-atom collisions at low energies. As stated in the Introduction the HSCC method has been used in many areas of three-body problems in atomic, molecular, and nuclear physics. The present implementation is targeted at systems with two heavy particles and a light one. This class of problems is characterized by the large momentum of the collision partners, and thus special care and approximations should be adopted before the HSCC method is used to obtain reaction cross sections at energies of interest.

In implementing the HSCC method for ion-atom collisions, we also adopted numerical technologies that have become available in the last two decades. We used the *B*-spline functions to solve the two-dimensional adiabatic hyperspherical channel functions. We also adopted the slow/smooth variable discretization technique and *R*-matrix propagation method to solve the hyperradial equation. Due to the rapid oscillations of the hyperradial wave functions, we modified the latter method with an interpolation procedure such that the number of hyperradial grid points where channel functions need to be calculated does not increase with collision energies. We also took advantage of the special properties of ion-atom collision systems such that the channel functions for the thousands of J's needed are calculated only once. These implementations make it possible to employ the HSCC method to treat ion-atom collisions over a broad range of energies.

We applied the HSCC method to obtain charge-transfer cross sections for the process $\mathrm{He}^{2+}+\mathrm{H}(1s)\rightarrow\mathrm{He}^{+}(n=2)+\mathrm{H}^{+}$ at center-of-mass energies below 4 keV. We presented our calculated charge-transfer cross sections. In the center-of-mass energy range between 10 and 200 eV, the total nonradiative charge-transfer cross section drops very rapidly with decreasing energies and our results agree with those from the distorted atomic orbital method of Fukuda and Ishihara [31], but not with the quantum molecular orbital calculations of van Hemert *et al.* At 200 eV, we showed that our partial wave cross sections also agree with the results of Fukuda and Ishihara.

We have extended the calculations to higher collision energies so that we can compare our results with those obtained using the semiclassical approximation and with experiments. Our results are slightly higher than the semiclassical calculations of Winter and Hatton [49], but both are within the experimental errors. We also compared our partial wave cross sections with their impact parameter dependent probabilities and there is a general agreement.

Our results clearly demonstrate that it is possible to employ the HSCC method to obtain cross sections for ion-atom collisions that have been traditionally treated using the so-called molecular orbital expansion method, but without the need to introduce *ad hoc* (or physically motivated) electron translational factors or switching functions. Further investigation of the HSCC method for other ion-atom collision systems is under way and extension to include more channels and at higher energies would allow us to probe the utility of this method. Careful comparison with molecular calculations based on reaction coordinates and/or switching functions for a number of collision systems is desirable to establish the region of validity of these MO-ETF-type calculations or calculations based on reaction coordinates. The latter methods are the standard approaches for treating many-electron ion-atom collision systems, and calculations based on the HSCC method for one-electron ion-atom collisions are desirable to provide theoretical data for comparison in view of the lack of accurate experimental data available for low-energy ion-atom collisions except for total charge-transfer cross sections.

ACKNOWLEDGMENTS

We thank Daiji Kato for providing the basic codes for *R*-matrix propagation. This work was supported in part by Chemical Sciences, Geosciences and Biosciences Division, Office of Basic Energy Sciences, Office of Science, U.S. Department of Energy. C.N.L. also acknowledges support from the National Science Council, Taiwan under Grant No. NSC 91-2119-M-009-002. T.M. acknowledges financial support from Grant-in-Aid for Scientific Research, Ministry of Education, Science and Culture, Japan.

[1] H. S. Massey and R. A. Smith, Proc. R. Soc. London, Ser. A **142**, 142 (1933).
[2] J. B. Delos, Rev. Mod. Phys. **53**, 287 (1981).
[3] B. H. Bransden and M. R. C. McDowell, *Charge Exchange and the Theory of Ion-Atom Collisions* (Clarendon, Oxford, 1992).
[4] A. Macias and A. Riera, Phys. Rep. **90**, 299 (1982).
[5] R. McCarroll and D. S. F. Crothers, Adv. At., Mol., Opt. Phys. **32**, 253 (1994).
[6] J. Grosser, T. Menzel, and A. K. Belyaev, Phys. Rev. A **59**, 1309 (1999).
[7] A. K. Belyaev, D. Egorova, J. Grosser, and T. Menzel, Phys. Rev. A **64**, 052701 (2001).
[8] W. R. Thorson and J. B. Delos, Phys. Rev. A **18**, 135 (1978).
[9] M. H. Mittleman, Phys. Rev. **188**, 221 (1969).
[10] M. Gargaud, R. McCarroll, and P. Valiron, J. Phys. B **20**, 1555 (1987).
[11] H. Croft and A. S. Dickinson, J. Phys. B **29**, 57 (1996).
[12] J. F. Castillo and L. Mendez, Phys. Rev. A **56**, 421 (1997).
[13] L. F. Errea, C. Harel, H. Jouin, L. Mendez, B. Pons, and A. Riera, J. Phys. B **31**, 3527 (1998).
[14] N. Shimakura and M. Kimura, Phys. Rev. A **44**, 1659 (1991).
[15] M. C. van Hemert, E. F. van Dishoeck, J. A. van der Hart, and F. Koike, Phys. Rev. A **31**, 2227 (1985).
[16] D. R. Bates and R. McCarroll, Proc. R. Soc. London, Ser. A **245**, 175 (1958).
[17] S. B. Schneiderman and A. Russek, Phys. Rev. **181**, 311 (1969).
[18] J. Vaaben and K. Taulbjerg, J. Phys. B **14**, 1815 (1981).
[19] C. D. Lin, Phys. Rep. **257**, 1 (1995).
[20] J. Tang, S. Watanabe, and M. Matsuzawa, Phys. Rev. A **46**, 2437 (1992).
[21] Y. Zhou and C. D. Lin, J. Phys. B **27**, 5065 (1994).
[22] P. Soldan, M. T. Cvita, J. M. Hutson, P. Honvault, and J. M. Launay, Phys. Rev. Lett. **89**, 153201 (2002).
[23] G. A. Parker, R. B. Walker, B. K. Kendrick, and R. T. Pack, J. Chem. Phys. **117**, 6083 (2002).
[24] A. Igarashi, I. Shimamura, and N. Toshima, Phys. Rev. A **58**, 1166 (1998).
[25] B. D. Esry, C. H. Greene, and J. P. Burke, Jr., Phys. Rev. Lett. **83**, 1751 (1999).
[26] J. Macek, M. Cavagnero, K. Jerjian, and U. Fano, Phys. Rev. A **35**, 3940 (1987).
[27] A. Igarashi and C. D. Lin, Phys. Rev. Lett. **83**, 4041 (1999).
[28] Z. X. Zhao, A. Igarashi, and C. D. Lin, Phys. Rev. A **62**, 042706 (2000).
[29] O. I. Tolstikhin, S. Watanabe, and M. Matsuzawa, J. Phys. B **29**, L389 (1996).
[30] D. Kato and S. Watanabe, Phys. Rev. A **56**, 3687 (1997).
[31] H. Fukuda and T. Ishihara, Phys. Rev. A **46**, 5531 (1994).
[32] A. K. Bhatia and A. Temkin, Rev. Mod. Phys. **36**, 1050 (1964).
[33] C. de Boor, *A Practical Guide to Splines* (Springer, New York, 1978).
[34] T. G. Heil, S. E. Butler, and A. Dalgarno, Phys. Rev. A **23**, 1100 (1981).
[35] P. C. Stancil, B. Zygelman, N. J. Clarke, and D. L. Cooper, Phys. Rev. A **55**, 1064 (1997).
[36] B. Zygelman, P. C. Stancil, N. J. Clarke, and D. L. Cooper, Phys. Rev. A **56**, 457 (1997).
[37] J. C. Light, I. P. Hamilton, and J. V. Lill, J. Chem. Phys. **82**, 1400 (1985).
[38] D. Skouteris, J. F. Castillo, and D. E. Manolopoulos, Comput. Phys. Commun. **133**, 128 (2000).
[39] K. Hino, A. Igarashi, and J. H. Macek, Phys. Rev. A **56**, 1038 (1997).
[40] K. L. Baluja, P. G. Burke, and L. A. Morgan, Comput. Phys. Commun. **27**, 299 (1982).
[41] O. I. Tolstikhin and H. Nakamura, J. Chem. Phys. **108**, 8899 (1998).

[42] J. C. Light and R. B. Walker, J. Chem. Phys. **65**, 4272 (1976).
[43] J. H. Macek, J. Phys. B **1**, 831 (1968).
[44] C. Greene, U. Fano, and G. Strinati, Phys. Rev. A **19**, 1485 (1979).
[45] C. R. Liu and A. F. Starace, Phys. Rev. A **40**, 4926 (1989).
[46] B. W. West, N. F. Lane, and J. S. Cohen, Phys. Rev. A **26**, 3164 (1982).
[47] K. Kobayashi, T. Ishihara, and N. Toshima, Muon Catal. Fusion **2**, 191 (1988).
[48] G. J. Hatton, N. F. Lane, and T. G. Winter, J. Phys. B **12**, L571 (1979).
[49] T. G. Winter and G. J. Hatton, Phys. Rev. A **21**, 793 (1980).
[50] L. F. Errea, J. M. Gomez-Llorente, L. Mendez, and A. Riera, J. Phys. B **20**, 6089 (1987).
[51] T. P. Grozdanov and E. A. Solov'ev, Phys. Rev. A **42**, 2703 (1990).